



A UAV-based framework for crop lodging assessment

Xiaohan Li ^a, Xuezhang Li ^b, Wen Liu ^{a,c,*}, Benhui Wei ^d, Xianli Xu ^b

^a College of Resources and Environmental Sciences, Hunan Normal University, Changsha 410125, China

^b Huanjiang Observation and Research Station for Karst Ecosystem, Key Laboratory for Agro-ecological Processes in Subtropical Region, Institute of Subtropical Agriculture, Chinese Academy of Sciences, Changsha 410125, China

^c Hunan Key Laboratory of Geospatial Big Data Mining and Application, Hunan Normal University, Changsha 410125, China

^d Cash Crops Research Institute, Guangxi Academy of Agricultural Sciences, Nanning 530007, China



ARTICLE INFO

Keywords:

Crop lodging assessment
UAV visible imagery
Feature selection
Boruta algorithm

ABSTRACT

Crop lodging assessment needs to be carried out timely and accurately to ensure valuable information about the location and area where lodging occurs. Many applications have been explored and tested for unmanned aerial vehicle (UAV) visible imagery in agricultural management due to the ability of providing high-space-resolution information. However, there still face many challenges in extracting lodging information using UAV visible imagery, and lacks consensus on an appropriate way to assess crop lodging. The main purpose of this study was to proposed an efficient framework to identify crop lodging at the field scale using UAV visible imagery. This framework contained a two-phase procedure. Meanwhile, three methods were evaluated by providing the appropriate feature subset for object-based classification to determine the best feature selection method. The results showed that the proposed framework provided high accuracy (94.0 %) for identification of sugarcane lodging. Furthermore, the Boruta algorithm yielded the best feature subset compared with statistical indicators and the RFE algorithm. Thus, the proposed framework based on UAV visible imagery is promising to identify crop lodging precisely, and has great application potential in precision agriculture.

1. Introduction

Crop lodging is the permanent displacement of a plant from its erect position and is seen as a main negative factor limiting harvest yield (Buitrago et al., 2000; Murakami et al., 2012). Lodging is prone to occur in numerous crop species. Among them, sugarcane (*Saccharum officinarum* L.) crops face high risk of lodging because of the plant's height and large above-ground biomass. Lodging is seriously harmful to sugarcane growth because it causes sugarcane roots to break, plants to dry out, and stems to turn over (Heerden et al., 2015; Li, 2019a). In addition, the sucrose content plunges, which makes it difficult to produce sugar and results in losses at sugar processing factories (Singh et al., 2002). Sugarcane, which contributes >90 % of the total sugar production in China every year (Li and Yang, 2015; Liang et al., 2020), is an important cash crop in southern China, where lodging frequently occurs due to extreme weather disasters, especially typhoons. Because the wind and rain that typhoons bring are the direct induction factors for lodging (Niu et al., 2016; Li, 2019a,b). Thus, carrying out crop lodging assessment is imperative to estimate the loss in disasters, predict the yield and improve crop management for farmers in agriculture production. The

traditional methods for identifying crop lodging were based on in situ assessments, which were inaccurate and inefficient due to the large area of farmland and manpower constraints (Han et al., 2018).

Remote sensing technology, which refers to the technique of acquiring information at a distance through specific sensors (Pajares, 2015), is a promising tool for monitoring crop growth and has been applied broadly in agricultural production in recent years. Satellite platforms offer continuous monitoring data with coverage from local to global. Unlike optical remote sensing data that is often restricted by meteorological conditions, synthetic aperture radar (SAR) data are preferable because they are free from clouds and rains (Wu et al., 2019; Yuan et al., 2019). Therefore, studies that focused on wheat, canola, and sugarcane have explored the potential capability of RADARSAT-2 data for monitoring crop lodging (Yang et al., 2015; Chen et al., 2016; Zhao et al., 2017). They found that the polarimetric features extracted from Polarimetric SAR data were sensitive to crop lodging, and they distinguished lodged plants from normal plants by comparing the polarimetric features before and after lodging. Another SAR data, Sentinel-1, was also used to assess the lodging of maize and corn (Han et al., 2017a; Shu et al., 2019). Moreover, Chauhan et al. (2020b) demonstrated that dense

* Corresponding author at: College of Resources and Environmental Sciences, Hunan Normal University, Changsha 410125, China.

E-mail address: liuwenww@gmail.com (W. Liu).

time series of high-resolution SAR data had the potential of estimating crop angle of inclination, which was a quantitative measure of lodging severity. However, a fixed revisit period, which each satellite platform included, sometimes caused satellite-based SAR data to be unable to provide timely data for crop lodging assessment (Chauhan et al., 2019a). Weather extremes, which might cause serious crop lodging, are always emergencies. The assessment of crop lodging needs to be carried out timely and accurately to guarantee information on the location and size of area in which lodging occurs.

Unmanned aerial vehicles (UAV), which are characterized by high flexibility and providing high-resolution spatial data, have been well developed and have great potential in precision agriculture (Freeman and Freeland, 2015). UAV systems are robust equipment that can be used to obtain images from low altitude so that images are not affected by cloud cover (Hung et al., 2014; De Castro et al., 2018). UAV systems are affordable and easily operated for advanced monitoring and site-specified management (Candago et al., 2015; Pajares, 2015; Luna and Lobo, 2016). A number of studies have investigated the potential for detecting crop lodging using a UAV system. Yang et al. (2017) established a comprehensive classification technique based on UAV imagery to assess rice lodging, and the lodging ratio at the study site was identified successfully. They also demonstrated that the classification technique was a promising tool with the inclusion of textural information and a digital surface model. In addition, a spatial and spectral hybrid analysis based on multispectral UAV images was conducted by Dai et al. (2019) to extract information about cotton lodging. They utilized two indices, coefficient of variation and relative difference, to extract useful features for classification between lodged cotton plants and normal plants with an accuracy of approximately 90 %. Liu et al. (2018) built a model to calculate lodging area using a combination of visible, textural, and thermal infrared images. The accuracy was >90 %. Furthermore, Rajapaksa et al. (2018) utilized texture features extracted from drone images of wheat and canola breeding plots to predict if lodging occurred and achieved 96.0 % accuracy for canola, and 92.6 % for wheat. Chauhan et al. (2019b) drew a conclusion that the magnitude of reflectance spectra would increase, especially in the bands of 700–950 nm, as the lodging became more severe through the analysis of multispectral data collected by UAV systems, and this could be effectively used to detect lodging in wheat.

The UAV system is advantageous for bridging the gap between ground-based surveys and conventional remote sensing data (Hall et al., 2018), because it allows for flexible data acquisition in the short term at low cost (Müllerová et al., 2017). However, conducting an assessment of crop lodging using UAV imagery still faces many challenges (Chauhan et al., 2019a). First, among most existing studies, the target area only included two types of objects, which were lodged plants and plants that were not lodged. But in practice, the research area is usually complicated and mixed by different crop species. It also includes artificial surfaces, such as roads and house roofs. Therefore, a two-step procedure is needed to identify the area of the target crop and then to assess the degree of lodging in the area. Second, while assessing crop lodging rapidly, the selection of a feature selection method is important because it will affect the classification outcome. Regardless of the datatypes used, the selection of optimal spectral bands (optical) or polarizations (radar) that are sensitive to lodging is challenging (Chauhan et al., 2019a; Wilke et al., 2019). Yet there has been little research that concentrated on feature selection, which is a crucial step in the procedure of assessing crop lodging. A feature selection algorithm aims at getting the best discriminating feature subset; an inappropriate feature subset may cause overfitting and inaccuracy in the results (Guyon and Elisseeff, 2003). Therefore, a robust feature selection algorithm is needed in the classification procedure.

In this study, we hypothesized that the proposed framework based on UAV visible imagery had the capacity of yielding enough accurate and reliable results to assess crop lodging. In order to examine that, this paper aimed to evaluate the performance of the proposed framework in

a case study of sugarcane lodging identification and make a comparison of three feature selection methods to determine the best methodology. The specific objectives are: (1) to construct a UAV-based framework which aimed first to identify the sugarcane field, and second to identify lodged sugarcane plants, and evaluate the accuracy; (2) to analyze the performances of three feature selection methods on identifying lodging-related features with the inclusion of textural information and visible vegetation indices.

2. Materials and methods

2.1. Study area

The experiment site was in Guangxi Zhuang Autonomous Region, southern China (Fig. 1). It was located in a low mountain and hill region, and the soil was primarily latosolic red soil. The climate in this region is characterized as a subtropical, monsoon, humid climate with annual precipitation of 1304.2 mm and an annual temperature of 21.6 °C. Sugarcane is one of the most important crops in this region, and the sugarcane variety was Guitang 42. According to the statistics of Guangxi Statistics Bureau, the size of the planting area of sugarcane in Guangxi was 886.40 Kha, and the production reached 73.97 million tons in 2018 (<http://tjj.gxzf.gov.cn/>), which ranked at the top in China.

This experiment was conducted on 19 September 2018, after Super Typhoon Mangkhut, the 22nd typhoon to hit the south of China in 2018. During September 16–18, precipitation was >100 mm, and the highest wind speed was nearly 45 m/sec in Guangxi (<http://www.weather.com.cn>). Based on the information from the sugar industry development office for the sugar industry, the lodging area was about 140 Kha in the entire province, of which 66 Kha were affected severely.

2.2. Framework

A framework was developed to identify sugarcane lodging based on the orthoimage collected using a UAV system after Super Typhoon Mangkhut (Fig. 2). Identification of sugarcane lodging occurred in two phases: (1) delimitation of sugarcane fields and other vegetation (which included alfalfa (*Medicago sativa L.*), banana (*Musa nana Lour.*), yam (*Dioscorea opposita Thunb.*), bare soil, etc.), and (2) identification of lodged sugarcane plants and undamaged sugarcane plants. Each phase used a binary classification procedure that was divided into four parts: (1) image segmentation, (2) feature selection, (3) object classification, and (4) accuracy assessment. In the first phase, sugarcane fields were identified separately from other vegetation fields in the study area. Next, we needed to discriminate the extent of lodged sugarcane plants from undamaged ones. Image segmentation was not needed in phase two because the orthoimage had been segmented before.

2.3. UAV imagery acquisition and mosaicking

High-resolution (0.9 m) images were collected by a DJI Phantom 3 Professional Edition (DJI Technology Co., Ltd., Shenzhen, China). Every photo had >70 % both forward overlap and side overlap to produce a high-quality orthoimage, which is critical for creating a mosaicked orthoimage (Lu and He, 2018). The flight height was 200 m above ground to cover all of the test sugarcane fields, and every flight mission was <20 min due to limited battery life.

After acquiring 236 images, Context Capture Master software (<http://www.bently.com>) was used to do aerial triangulation and mosaicking for an orthoimage of the entire area. There was no ground control point used in this study because the GPS and global navigation satellite system (GLONASS) on-board the UAV provided enough information for aerial triangulation.

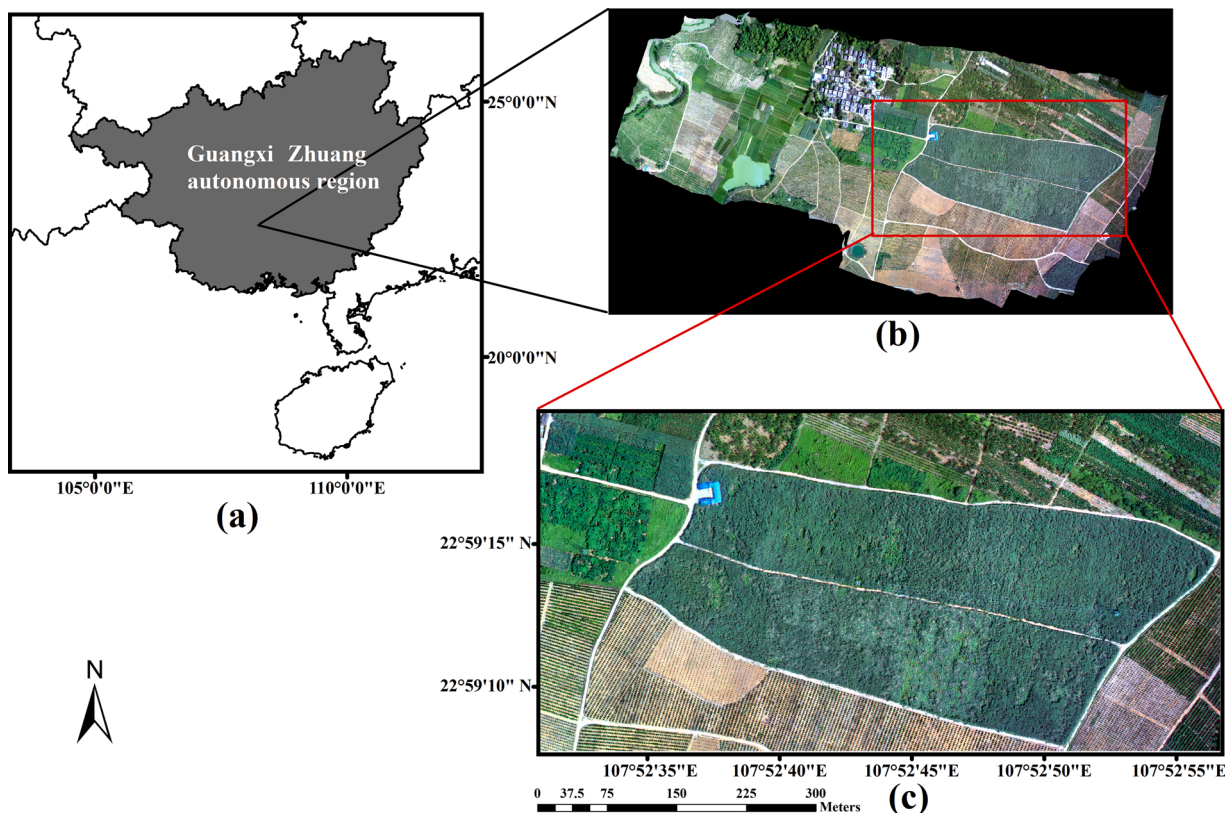


Fig. 1. (a) The location of the study area within China. (b) The orthoimage of the study area captured by the UAV system (taken on 19 September 2018). (c) The study area (image taken at 200 m altitude).

2.4. Image segmentation

Segmentation refers to the process of dividing an image into several objects, which act as the units of classification instead of conventional pixels. In object-based image analysis (OBIA) technology, high-resolution images are first segmented into many single objects that merge homogeneous and adjacent pixels, and all objects are classified next. This simplifies the representation of an image into a more meaningful and homogeneous structure that makes it easier to describe the properties of each object (Ruiz et al., 2011; Duro et al., 2012), because using high-space-resolution images to identify sugarcane lodging may cause severe salt-and-pepper noise that results from high in-class variability due to gaps or shadows (Akar, 2018). To overcome this kind of noise, in this study, orthoimages were segmented by the multiresolution segmentation algorithm (MRSA) in eCognition Developer 9.0 software (Trimble Germany GmbH, Munich, Germany). MRSA is a bottom-up segmentation technique, which means that it merged single pixels into larger segments and utilized spatial heterogeneity differences to control the size of image objects (Cleve et al., 2008). Three parameters should be given here: scale, shape, and compactness. Scale controlled the average size of each object. Shape and color were weighted in a range from zero to one. Likewise, compactness and smoothness, which made up the shape setting, were from zero to one. This step was processed before phase one. The segmentation scale was set as 80, and shape and compactness were both 0.5.

2.5. Feature selection

In OBIA, one of the main challenges is to determine suitable features for classification. In this study, there were three kinds of features derived from image objects (Table 1). The first was the mean band value, which included red, green, and blue. The second was the visible band vegetation index. Five visible vegetation indices were chosen as features for

classification, which included visible-band difference vegetation index (VDVI), modified green red vegetation index (MGRVI), green-red vegetation index (GRDI), green-blue vegetation index (GBVI), and excess green (EXG) (Bendig et al., 2015; Wang et al., 2015; David and Ballado, 2016). The third was the textural feature. Textural features are statistical measures of structure that are defined as smooth when the within-class variability was lower than the between-class variability (Laliberte and Rango, 2009; Wang et al., 2015). The most popular method to do textural analysis is the gray level co-occurrence matrix (GLCM), and eight variables were extracted to assist in classification: mean (MEAN), variance (VAR), homogeneity (HOM), contrast (CON), dissimilarity (DIS), entropy (ENT), angular second moment (ASM), and correlation (COR) (Haralick et al., 1973).

Samples were needed for feature selection. In the study area, there were mainly three types of objects that we needed to identify: sugarcane, other vegetation (alfalfa, banana, etc.), and artificial surfaces. Artificial surfaces could be extracted rapidly by setting a threshold value for the blue band. For the other features, training samples were needed to train a classification model, and test samples were needed to evaluate the efficiency of this model. The process in each phase was a binary classification, so only two categories were needed. Eighty sugarcane objects and 80 other vegetation objects were chosen as training samples in phase one, and 25 lodged sugarcane objects and 25 normal sugarcane objects were used in phase two.

Feature selection was processed using an object-based classification procedure because the feature subset needed to be optimized to have high in-class similarity and low inter-class overlap (Ma et al., 2017). In our study, three feature selection methods were utilized to make a comparison: statistical indicators, the recursive feature elimination (RFE) algorithm, and the Boruta algorithm.

For using statistical indicators in feature selection, two indicators, which could be calculated to describe the separability of the sample set, were chosen: coefficient of variance (CV) and relative difference (RD)

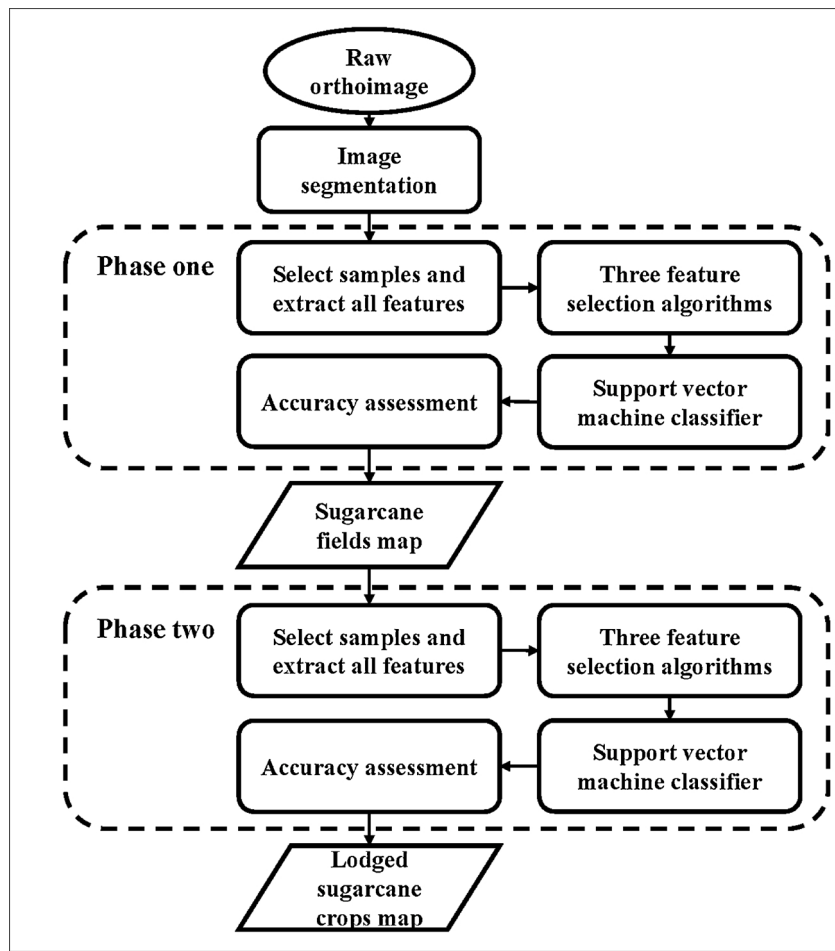


Fig. 2. Proposed framework using UAV imagery.

Table 1

The features and corresponding formulas for classification. R , G , and B are the pixel values of bands red, green, and blue, respectively, and r , g , and b are the normalized pixel values of bands red, green, and blue, respectively. ρ is the band value. P_{ij} is the normalized co-occurrence matrix. N is the number of rows or columns. σ_i and σ_j are the standard deviation of row i and column j . μ_i and μ_j are the mean of row i and column j .

Feature name	Formula	Feature name	Formula
Red	Mean value of R band	MEAN	$\frac{\sum_{i,j=0}^{N-1} P_{ij}}{N^2}$
Green	Mean value of G band	HOM	$\frac{\sum_{i,j=0}^{N-1} P_{ij}}{1 + (i-j)^2}$
Blue	Mean value of B band	CON	$\frac{\sum_{i,j=0}^{N-1} P_{ij}(i-j)^2}{\sum_{i,j=0}^{N-1} P_{ij}}$
EXG	$2g - r - b$	DIS	$\frac{\sum_{i,j=0}^{N-1} P_{ij} i-j }{\sum_{i,j=0}^{N-1} P_{ij}}$
NGRVI	$\frac{G-R}{G+R}$	COR	$\frac{\sum_{i,j=0}^{N-1} P_{ij}(i-\mu_i)(j-\mu_j)}{\sigma_i \sigma_j}$
MGRVI	$\frac{G^2 - R^2}{G^2 + R^2}$	EN	$\frac{\sum_{i,j=0}^{N-1} P_{ij}(-\ln P_{ij})}{\sum_{i,j=0}^{N-1} P_{ij}}$
NGBVI	$\frac{G-B}{G+B}$	ASM	$\frac{\sum_{i,j=0}^{N-1} P_{ij}^2}{\sum_{i,j=0}^{N-1} P_{ij}}$
VDDVI	$\frac{2G-R-B}{2G+R+B}$	VAR	$\sqrt{\sum_{i,j=0}^{N-1} P_{ij}(i-\mu_i)^2} \cdot \sqrt{\sum_{i,j=0}^{N-1} P_{ij}(i-\mu_j)^2}$ where $\sigma_i^2 = \sum_{i,j=0}^{N-1} P_{ij}(i-\mu_i)^2$,

(Table 2) (Han et al., 2017b; Dai et al., 2019). The coefficient of variance reflected the degree of sample dispersion in one class and, when it was small, the feature tended to be unique and well characterized. The

Table 2

Statistical indicators for feature selection. D is the standard deviation and M is the mean value calculated from samples.

Statistical indicator	Formula
Coefficient of variance	$CV = \frac{D}{M} \times 100\%$
Relative difference	$RD = \frac{M_1 - M_2}{M_2} \times 100\%$

relative difference reflected the difference between two classes, and it was easier to distinguish one class from another when RD was larger. We set a criterion of <15 % in CV and >10 % in RD for selecting the feature subset.

The recursive feature elimination (RFE) algorithm is a wrapper-based algorithm that is embedded in the package ‘caret’ in R (Max, 2008). It is a recursive process that ranks all features according to their importance and removes the less relevant ones iteratively based on a Random Forest model. In the end, the model identifies one feature subset with the best accuracy and the smallest size.

The Boruta algorithm was run using R (<https://www.r-project.org/>). This algorithm is also a wrapper algorithm based on Random Forest that finds all relevant variables for classification (Kursa and Rudnicki, 2010). ‘Shadow features’ were introduced in it by shuffling the original feature set randomly, and then Boruta calculated the Z-scores, which represented the importance of features. When the Z-score of one of the original features was lower than the largest Z-score of some ‘shadow feature’, this original feature was considered ‘unimportant’ and removed due to its irrelevance to classification. Therefore, all variables

that made a positive contribution to classification, even if very small, remained.

2.6. Object-based classification

For object-based classification, there were many potential classifiers. However, regardless of the selected classifiers, object-based classification presents two main challenges: linear non-separability and class imbalance (Chen et al., 2011). Considering this, a supervised learning classifier called support vector machine (SVM) was used due to its advantages in solving linear non-separability. It aimed to process in a high dimension space that was established by all given features, and it mapped all the samples to this space. It tended to create many hyperplanes for classification that created a large distance between two categories. For this study, a radial basis function (RBF) kernel was used. Two parameters used in the RBF kernel were “Cost” (C) and “Sigma” (σ). C ranged from 1 to 10000, and σ ranged from 0.0001 to 0.1. Through tuning parameters, we identified the strongest parameters for the SVM classifier. C equaled to 1 and σ equaled to 0.01 in phase one, and C equaled to 10 and σ equaled to 0.001 in phase two.

2.7. Accuracy assessment

A confusion matrix was used to conduct an accuracy assessment for the classifications. A test set was selected according to the classifications, which included real samples based on in situ research and test samples based on the framework in this paper. The classification accuracy was evaluated using two main measures: overall accuracy (OA) and the Kappa coefficient. OA was determined by dividing the total correct pixels by the total number of pixels in the confusion matrix, and Kappa was a measure of agreement or accuracy between the remote sensing classification map and the ground truth data.

3. Results

3.1. Feature selection

3.1.1. Statistical indicators calculated in both phases

There was a total of 32 features, which included three band values, five visible band vegetation indices, and 24 textural features, and the results of each feature were calculated to select fitting features (Table 3). According to the aforementioned criterion in Section 2.5 (i.e., a CV < 15 % and a RD > 10 %), 13 of the 32 features were selected for phase one, which included G_ASM, R_ASM, B_ASM, NGRVI, G_HOM, VDVI, B_HOM, B_EN, MGRVI, NGBVI, G_DIS, B_DIS, and R_MEAN. Five features

Table 3

The results of statistical indicators based on the test samples in phase one. The bolded features remained for object-based classification, and the unbolded ones were eliminated.

Feature	CV (%)	RD (%)	Feature	CV (%)	RD (%)
G_ASM	0.08	25.20	R_DIS	2.65	7.59
R_ASM	0.09	11.40	G_DIS	3.27	14.35
B_ASM	0.13	31.55	B_DIS	4.12	25.74
G_COR	0.16	4.34	B_MEAN	6.56	0.33
R_HOM	0.26	0.23	G_MEAN	9.42	6.43
B_COR	0.26	2.60	R_MEAN	12.98	21.28
NGRVI	0.26	343.60	Blue	28.53	0.09
G_EN	0.30	6.76	Green	39.21	6.76
G_HOM	0.30	10.42	R_CON	41.24	24.85
R_COR	0.31	9.85	R_VAR	48.96	49.97
VDVI	0.32	44.52	G_CON	49.13	19.46
R_EN	0.33	2.13	Red	53.03	21.44
B_HOM	0.34	13.08	G_VAR	54.25	3.94
B_EN	0.49	10.66	B_CON	118.00	45.48
MGRVI	0.51	347.48	B_VAR	133.04	22.25
NGBVI	1.57	60.71	EXG	133.64	91.95

Table 4

The results of statistical indicators based on the test samples in phase two. The bolded features remained for object-based classification, and the unbolded ones were eliminated.

Feature	CV (%)	RD (%)	Feature	CV (%)	RD (%)
G_ASM	0.09	6.77	B_DIS	2.14	10.40
G_COR	0.09	6.95	R_DIS	2.29	2.29
R_ASM	0.09	1.72	G_DIS	2.88	7.15
R_COR	0.15	9.94	B_MEAN	6.22	4.74
B_ASM	0.15	9.58	G_MEAN	8.71	7.36
B_COR	0.19	8.84	R_MEAN	11.99	11.84
R_HOM	0.25	1.95	B_CON	18.13	16.67
B_HOM	0.28	6.27	B_VAR	20.14	1.57
G_EN	0.29	1.44	Blue	25.42	4.75
R_EN	0.29	0.17	R_CON	25.47	3.13
G_HOM	0.29	5.36	G_CON	33.82	12.74
NGRVI	0.30	22.96	Green	36.65	7.36
VDVI	0.39	5.50	R_VAR	36.92	22.75
B_EN	0.47	2.25	G_VAR	40.72	1.67
MGRVI	0.58	22.77	Red	49.23	11.78
NGBVI	1.04	56.42	EXG	166.49	1.24

(Table 4) were collected for phase two under the same criterion: NGRVI, MGRVI, NGBVI, B_DIS, and R_MEAN.

3.1.2. RFE algorithm for finding the minimal, optimal feature subsets

Each feature was evaluated quantitatively for its importance and then was introduced in decreasing order of importance to determine classification accuracy. The accuracy was highest (classification accuracy: 98.2 %; Kappa: 0.96) when we included the first seven features (the smallest) (Fig. 3(a)). This was the minimal, optimal feature subset created by the RFE algorithm that included B_MEAN, Blue, B_ASM, R_VAR, B_EN, NGRVI, and MGRVI. Likewise, 12 features were selected as one feature subset (classification accuracy: 93.6 %; Kappa: 0.87) in phase, (Fig. 3(b)) which included R_COR, Red, R_MEAN, NGRVI, MGRVI, G_COR, B_COR, G_MEAN, Green, R_VAR, B_ASM, and Blue.

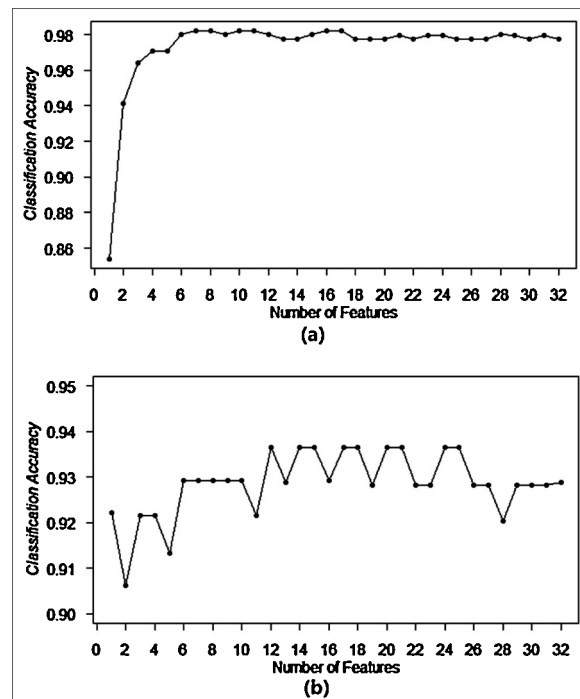


Fig. 3. The results of the recursive feature elimination algorithm in phase one (a) and phase two (b). Classification accuracy with the introduction of features from most to least important. By the end, one feature subset remained that had the highest accuracy and the smallest size for object-based classification.

3.1.3. The Boruta algorithm for finding all relevant feature subsets

The results of the Boruta algorithm were presented through two box diagrams. In phase one, there were no features eliminated because all features were positive for classification (Fig. 4(a)). In phase two, seven features were eliminated, which included B_VAR, R_CON, R_HOM, G_VAR, R_ASM, R_DIS, and VDVI. The remaining 25 features were selected as one feature subset (Fig. 4(b)).

3.2. Classification results

The three feature selection methods gave completely different results when trained by the same samples in each phase (Tables 5 and 6). A comparison between methods was done to evaluate the suitability for classification in the framework we proposed for phase one (Fig. 5). By comparing with the raw image visually, the Boruta algorithm clearly yielded the closest result to the real distribution of sugarcane fields.

The raw data for phase two was from the result using the Boruta algorithm in phase one (Fig. 5(d)) because that method showed the highest classification accuracy and highest Kappa coefficient. Additionally, although the Boruta algorithm gave the best result in phase one, we still used all three feature selection methods in phase two as a way to verify the stability of each method. There were few differences between the results from the three methods that were tested in phase two, however, the Boruta algorithm gave the closest result to reality (Fig. 6). As determined by crop mapping after classification in this study, the sugarcane fields covered an area of 11.72 ha. The whole area of lodging in sugarcane fields occupied 2.51 ha, which covered 21.4 % of the area planted with sugarcane.

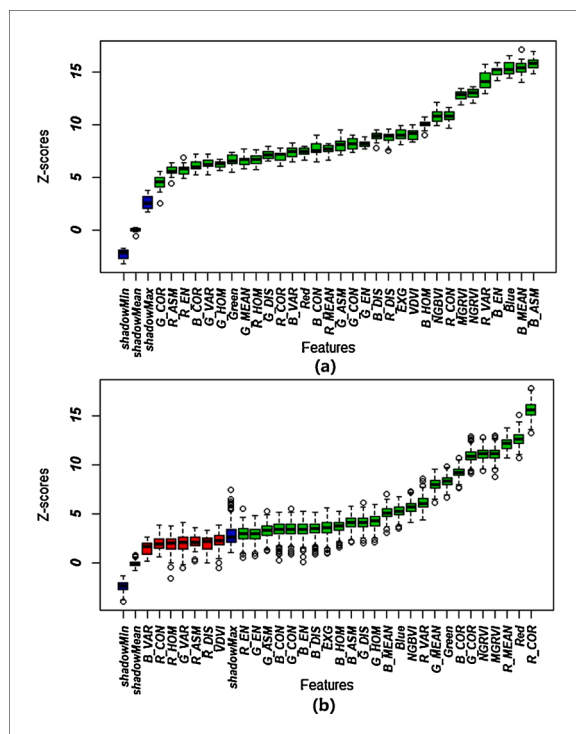


Fig. 4. Feature selection based on the Boruta algorithm in (a) phase one and (b) phase two. Blue features are 'shadow features'. Green features remained at the end of the phases and were a part of the object-based classification. Red features were eliminated as less important than 'shadow features'. The importance of each feature increases from left to right. According to the results, all 32 features remained in phase one, and seven features were eliminated in phase two (For interpretation of the references to colour in this figure legend, the reader is referred to the web version of this article).

Table 5

The results of feature selection in phase one given by three feature selection methods.

Method	Result	Number of features
Statistical indicators	G_ASM, R_ASM, B_ASM, NGRVI, G_HOM, VDVI, B_HOM, B_EN, MGRVI, NGBVI, G_DIS, B_DIS, R_MEAN	13
RFE algorithm	B_MEAN, Blue, B_ASM, R_VAR, B_EN NGRV, MGRVI;	7
Boruta algorithm	All 32 features	32

Table 6

The results of feature selection in phase two given by three feature selection methods.

Method	Result	Number of features
Statistical indicators	NGRVI, MGRVI, NGBVI, B_DIS, R_MEAN;	5
RFE algorithm	R_COR, Red, R_MEAN, NGRVI, MGRVI, G_COR, B_COR, G_MEAN, Green, R_VAR, B_ASM, Blue;	12
Boruta algorithm	R_COR, Red, R_MEAN, MGRVI, NGRVI, G_COR, B_COR, Green, G_MEAN, R_VAR, NGBVI, Blue, B_MEAN, G_HOM, G_DIS, B_ASM, B_HOM, EXG, B_DIS, B_EN, G_CON, B_CON, G_ASM, G_EN, R_EN;	25

3.3. Accuracy assessment

To conduct a quantitative assessment of classification accuracy, 160 test objects were chosen randomly for phase one, and 50 were chosen for phase two as test samples. Test samples were independent from training samples, and two confusion matrices were built using the test samples. The feature subset from the Boruta algorithm (Table 7) presented the highest OA (98.7 %) and Kappa coefficient (0.97). This was the best result in phase one. For other methods, the errors in classification occurred mainly because many sugarcane objects were misclassified into other vegetation objects. The Boruta algorithm had the best overall accuracy (OA = 94.0 %) and Kappa coefficient (0.88) (Table 8). Consequently, the Boruta algorithm performed best in both phases, but classification based on statistical indicators had the worst overall accuracy and lowest Kappa coefficient.

4. Discussion

In this study, the framework for sugarcane lodging assessment based on UAV RGB imagery was established and tested. The results showed that the extent and the ratio of lodged sugarcane plants in our study area could be determined reliably and accurately with a two-phase classification strategy and an appropriate feature selection method.

Among previous studies on identification of crop lodging, feature selection was always a research focus because selection of the features that were sensitive to lodging was key to improving accuracy. For the spectral and textural features considered in this study, the Boruta algorithm output the best features for identification of sugarcane lodging. The Boruta algorithm was relatively stable and robust because the algorithm found all features that were relevant to classification even when the relationship to classification was small (Kursa and Rudnicki, 2010), which was why this method tended to acquire higher classification accuracy than other methods when we used the same samples for training. Agjee et al. (2016) also showed that the Boruta algorithm produced fewer classification errors than the RFE algorithm in species classification. Moreover, in addition to the better performance of the Boruta algorithm, higher accuracy was also obtained due to the set of training samples with abundant information. It was important to note that the

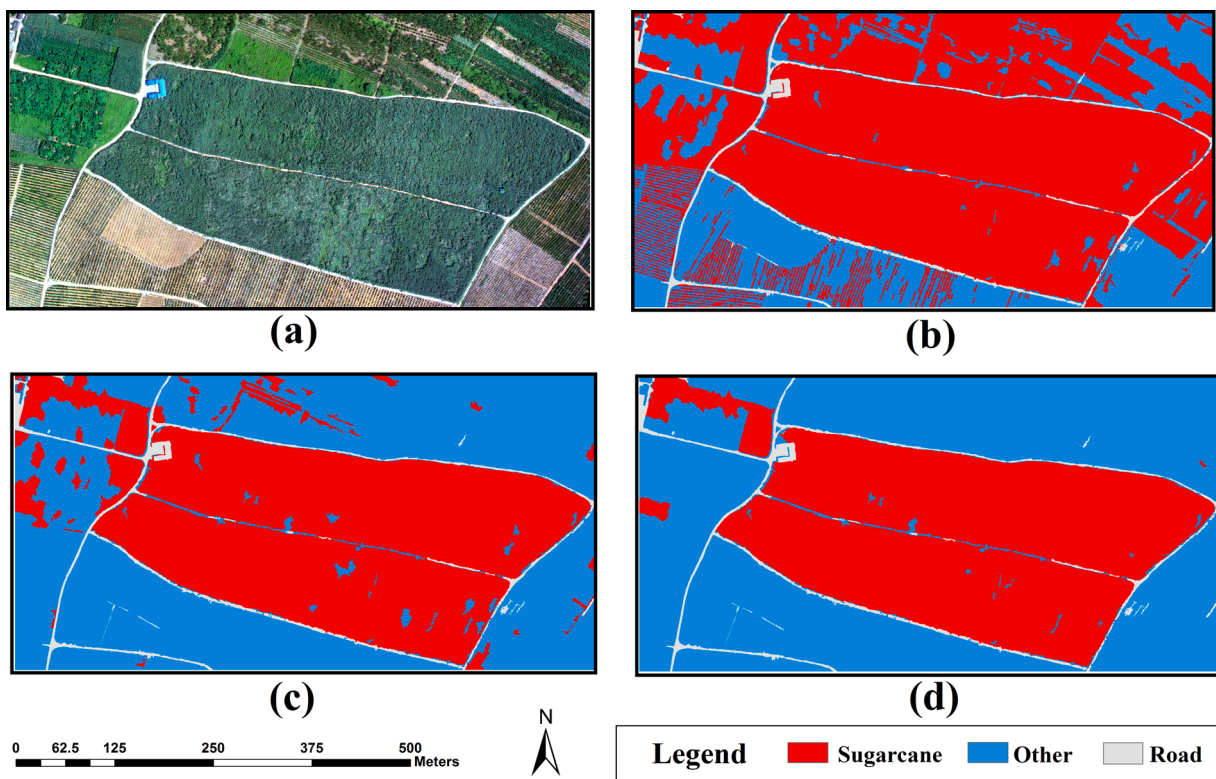


Fig. 5. (a) The raw image presented the real spatial distribution of sugarcane fields. Object-based classification results in phase one based on (b) the statistical indicators, (c) the RFE algorithm, and (d) the Boruta algorithm.

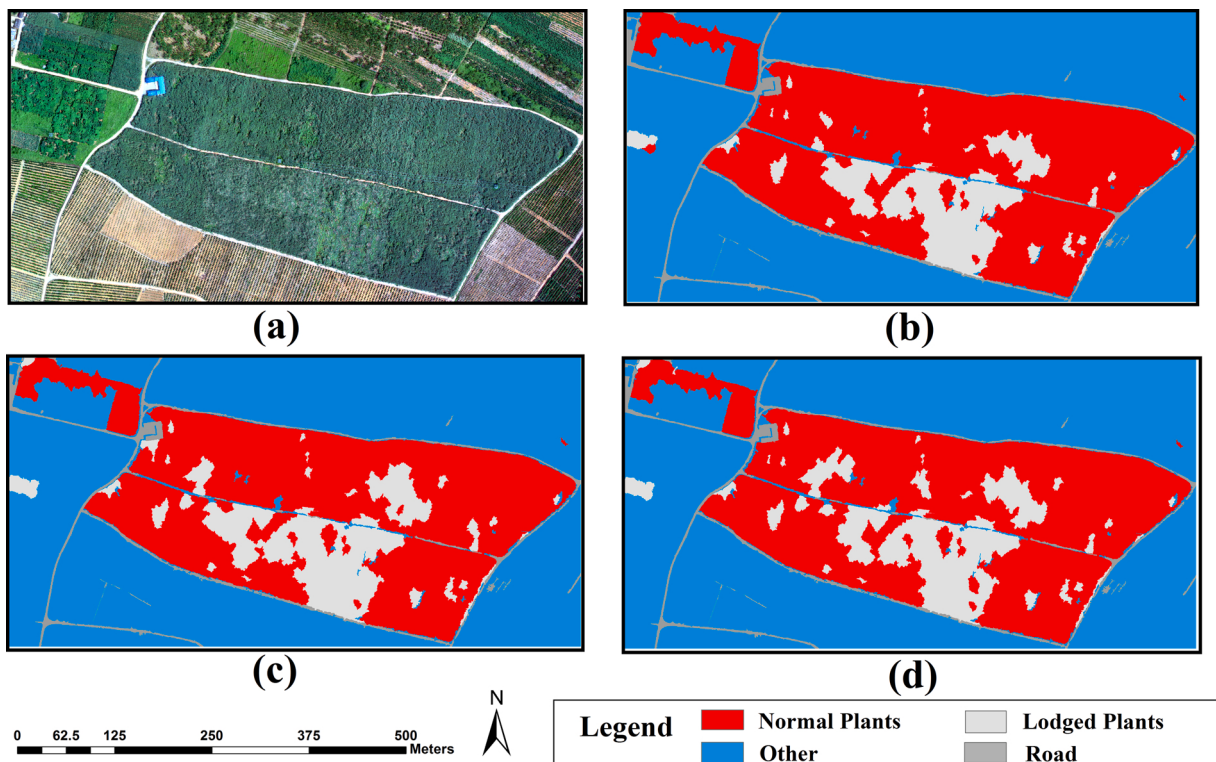


Fig. 6. (a) The raw image presented the real spatial distribution of lodged sugarcane crops. Object-based classification results in phase two based on (b) the statistical indicators, (c) the RFE algorithm, and (d) the Boruta algorithm. The raw image for phase two came from Fig. 5 (d) because it had the highest accuracy in phase one.

Table 7

Confusion matrices of the three object-based classification results according to the same test samples between sugarcane fields and other vegetation in phase one.

	Statistical indicators			RFE algorithm			Boruta algorithm		
	Sugarcane	Other	Sum.	Sugarcane	Other	Sum.	Sugarcane	Other	Sum.
Sugarcane	78	50	128	77	9	86	79	1	80
Other	2	30	32	3	71	74	1	79	80
Sum.	80	80		80	80		80	80	
OA	66.9 %			92.5 %			98.7 %		
Kappa	0.34			0.85			0.97		

Table 8

Confusion matrices of the three object-based classification results based on the same test samples between lodged sugarcane crops and normal ones in phase two.

	Statistical indicators			RFE algorithm			Boruta algorithm		
	Lodged	Normal	Sum.	Lodged	Normal	Sum.	Lodged	Normal	Sum.
Lodged	19	1	20	21	1	22	23	1	24
Normal	6	24	30	4	24	28	2	24	26
Sum.	25	25		25	25		25	25	
OA	86.0 %			90.0 %			94.0 %		
Kappa	0.73			0.80			0.88		

higher the amount of input data there was, the better was the effect that we achieved (Zhao et al., 2019). In phase one, in which we distinguished sugarcane fields over other vegetation, the selection of training samples was very complicated because many different kinds of crops were cultivated in our study area, which included sugarcane, alfalfa, banana, etc., and there were also artificial surfaces. To exclude non-sugarcane areas, training samples needed to ensure that all kinds of objects mentioned above were included. Otherwise, the probability of an error in the classification model increased. In this study, all samples were selected based on field investigations rather than visual interpretation of imagery to ensure accuracy. Therefore, the results of this study indicated that relatively high classification accuracy using UAV RGB imagery was achieved with the use of abundant training samples and an appropriate feature selection method.

The images of sugarcane fields in this study were obtained using a high-resolution digital camera with only three bands that included red, blue, and green. Thus, only spectral and textural features were extracted from RGB imagery. However, Liu et al. (2018) did a quantitative analysis and found that the differences in single spectral or textural features were not sufficient for lodging recognition. They combined thermal infrared devices with UAV systems and utilized the temperature difference between lodged rice plants and non-lodged plants. Chapman et al. (2014) concluded that lodged areas were detected better using surface temperatures so that thermal imagers were better for identifying lodged areas. Moreover, Yang et al. (2015) and Chauhan et al. (2020a) both deemed that the polarimetric parameters were sensitive to crop lodging, so they successfully used the polarimetric features extracted from SAR data to classify and assess wheat lodging. These studies proved that their methods worked in identifying crop lodging.

Nevertheless, these methods still faced a few limitations on guarantee timely information. Liu et al. (2018) suggested that the temperature difference was significant from 10 a.m. to 4 p.m. on sunny days so that only this period was optimal for monitoring crop lodging. Additionally, satellite-based data, which included both optical and SAR data, were more suitable for monitoring seasonal lodging or for mapping the risk of lodging on a large scale. But it was less effective for post-disaster lodging assessment due to a fixed revisit period. The UAV system could provide more timely and precise information compared with satellite platforms (Liu et al., 2014; Aasen et al., 2015), and the incorporation of spectral and textural features significantly improved the accuracy of identification (Laliberte and Rango, 2009; Kim et al., 2011), even though textural features were highly related to image resolution and quality (Pacifici et al., 2009). Therefore, UAV RGB imagery has significant practical value for real applications currently, and it is

consumer-friendly at the same time. Mardanisamani et al. (2019) established a deep convolutional neural network for lodging prediction using an RGB orthoimage and validated that lodging detection could be carried out with high accuracy even in the absence of red edge and near-infrared channels. In our study, with an appropriate feature selection method, the results suggested that the combination of spectral and textural features was enough to identify sugarcane lodging because the accuracy achieved 94 %. If conditions are suitable in future studies, thermal infrared or radar devices can be combined with UAV systems and, thus, temperature or polarimetric features can be analyzed using feature selection methods with spectral and textural features simultaneously to explore which features are suitable for identification of crop lodging.

5. Conclusions

In this study, the results validated the hypothesis that the two-phase framework we constructed was capable of yielding a reliable and accurate result for crop lodging assessment using UAV visible imagery and an appropriate feature selection method. First, the overall accuracy of lodged sugarcane plants identification achieved 94.0 % using UAV visible imagery. The two-step strategy also overcame the problem that the research area was mixed by multiple crop species and reduce the probability of the classification error caused by the phenomenon of "similar spectrum from different objects". Second, the Boruta algorithm produced the best feature subset with the accuracy of 98.7 % in phase one, and 98.0 % in phase two. The overall accuracies demonstrated that the Boruta algorithm could effectively extract lodging-related features within 32 default features compared with the other tested methods. It also suggested that selecting a robust feature selection method could significantly improve classification accuracy. Moreover, the framework proposed in this study provided high practical value and could meet the demand for identifying specific locations and spatial areas of lodged crops at the field scale. A robust feature selection algorithm could ensure the ability of detecting the changes between lodged plants and non-lodged ones using the combination of multiple features. The OBIA technology and the SVM classifier provided effective classification procedure using high-space-resolution imagery. Therefore, the proposed framework had great application potential in monitoring crop lodging at the field scale.

However, it was still worth noting that the results of the framework were limited by the selection of the training samples. Each crop species in the study area needed to be ensured in the training samples so as to minimize the probability of an error in the classification, which required

detailed ground investigation. In future research, more types of features, such as temperature or polarimetric features, need to be considered in feature selection to determine which features are more suitable for assessing crop lodging. Furthermore, it is necessary to explore the method of real-time or automatic lodging monitoring based on the framework we proposed.

CRediT authorship contribution statement

Xiaohan Li: Conceptualization, Methodology, Investigation, Writing - original draft. **Xuezhang Li:** Investigation, Resources, Validation, Writing - review & editing. **Wen Liu:** Validation, Supervision. **Benhui Wei:** Project administration, Funding acquisition. **Xianli Xu:** Conceptualization, Supervision, Project administration, Funding acquisition, Writing - review & editing.

Declaration of Competing Interest

The authors declare that they have no known competing financial interests or personal relationships that could have appeared to influence the work reported in this paper.

Acknowledgments

This study was financially supported by the Science and Technology Major Project of Guangxi (GuikeAA17204037), National Natural Science Foundation of China (Nos. 41977014; 41601223; 41571130073), Guangxi Natural Science Foundation (2018GXNSFBA294010), National Key Research and Development Program of China (2019YFE0116900), CAS Interdisciplinary Innovation Team, and the Youth Innovation Team Project of ISA, CAS (2017QNCXTD XXL).

References

- Aasen, H., Burkart, A., Bolten, A., Bareth, G., 2015. Generating 3D hyperspectral information with lightweight UAV snapshot cameras for vegetation monitoring: from camera calibration to quality assurance. *ISPRS J. Photogramm. Remote. Sens.* 108, 245–259. <https://doi.org/10.1016/j.isprsjprs.2015.08.002>.
- Agjee, N.E., Ismail, R., Mutanga, O., 2016. Identifying relevant hyperspectral bands using Boruta: a temporal analysis of water hyacinth biocontrol. *J. Appl. Remote Sens.* 10, 042002–042018. <https://doi.org/10.1117/1.JRS.10.042002>.
- Akar, Ö., 2018. The rotation forest algorithm and object based classification method for land use mapping through UAV images. *Geocarto Int.* 33, 538–553. <https://doi.org/10.1080/10106049.2016.1277273>.
- Bendig, J., Yu, K., Aasen, H., Bolten, A., Bennertz, S., Broscheit, J., Gnyp, M., Bareth, G., 2015. Combining UAV-based plant height from crop surface models, visible, and near infrared vegetation indices for biomass monitoring in barley. *Int. J. Appl. Earth Obs. Geoinf.* 39, 79–87. <https://doi.org/10.1016/j.jag.2015.02.012>.
- Buitrago, J.T., Amaya, A., Gomez, A., Moreno, C., Cassalotti, C., Characterization of lodging in sugarcane, 2000. 2000 22nd Australian Society of Sugarcane Technologists Conference, pp. 321–327.
- Candiago, S., Remondino, F., De Giglio, M., Dubbini, M., Mario, G., 2015. Evaluating multispectral images and vegetation indices for precision farming applications from UAV images. *Remote Sens.* 7, 4026–4047. <https://doi.org/10.3390/rs70404026>.
- Chapman, S., Merz, T., Chan, A., Jackway, P., Hrabar, S., Drecer, M., Holland, E., Zheng, B., Ling, T., Berni, J., J.A., 2014. Pheno-copter: a low-altitude, autonomous remote-sensing robotic helicopter for high-throughput field-based phenotyping. *Agronomy* 4, 279–301. <https://doi.org/10.3390/agronomy4020279>.
- Chauhan, S., Darvishzadeh, R., Boschetti, M., Pepe, M., Nelson, A., 2019a. Remote sensing-based crop lodging assessment: current status and perspectives. *Isprs J. Photogramm. Remote. Sens.* 151, 124–140. <https://doi.org/10.1016/j.isprsjprs.2019.03.005>.
- Chauhan, S., Darvishzadeh, R., Lu, Y., Stroppiana, D., Boschetti, M., Pepe, M., Nelson, A., 2019b. Wheat lodging assessment using multispectral UAV data. *ISPRS - international archives of the photogrammetry, Remote Sens. Spatial Inf. Sci.* XLII-2/W13, 235–240. <https://doi.org/10.5194/isprs-archives-XLII-2-W13-235-2019>.
- Chauhan, S., Darvishzadeh, R., Boschetti, M., Nelson, A., 2020a. Discriminant analysis for lodging severity classification in wheat using RADARSAT-2 and Sentinel-1 data. *ISPRS J. Photogramm. Remote. Sens.* 164, 138–151. <https://doi.org/10.1016/j.isprsjprs.2020.04.012>.
- Chauhan, S., Darvishzadeh, R., Boschetti, M., Nelson, A., 2020b. Estimation of crop angle of inclination for lodged wheat using multi-sensor SAR data. *Remote Sens. Environ.* 236, 111488–111502. <https://doi.org/10.1016/j.rse.2019.111488>.
- Chen, X., Fang, T., Huo, H., Li, D., 2011. Graph-based feature selection for object-oriented classification in VHR airborne imagery. *IEEE Trans. Geosci. Remote. Sens.* 49, 353–365. <https://doi.org/10.1109/TGRS.2010.2054832>.
- Chen, J., Li, H., Han, Y., 2016. Potential of RADARSAT-2 data on identifying sugarcane lodging caused by typhoon. 2016 5th International Conference on Agro-Geoinformatics (Agro-Geoinformatics) 1–6. <https://doi.org/10.1109/Agro-Geoinformatics.2016.7577665>.
- Cleve, C., Kelly, M., Kearns, F., Moritz, M., 2008. Classification of the wildland–urban interface: a comparison of pixel- and object-based classifications using high-resolution aerial photography. *Comput. Environ. Urban Syst.* 317–326. <https://doi.org/10.1016/j.compenvurbsys.2007.10.001>.
- Dai, J., Zhang, G., Guo, P., Zeng, T., Cui, M., Xue, J., 2019. Information extraction of cotton lodging based on multi-spectral image from UAV remote sensing. *Trans. Chin. Soc. Agric. Eng.* 35, 63–70. <https://doi.org/10.11975/j.issn.1002-6819.2019.02.009>.
- David, L., Ballado, A., 2016. Vegetation indices and textures in object-based weed detection from UAV imagery. 2016 6th IEEE International Conference on Control System, Computing and Engineering (ICCSCE) 273–278. <https://doi.org/10.1109/ICCSCE.2016.7893584>.
- De Castro, A., Torres-Sánchez, J., Peña-Barragán, J.M., Jiménez-Brenes, F., Csillik, O., López-Granados, F., 2018. An automatic random forest-OBIA algorithm for early weed mapping between and within crop rows using UAV imagery. *Remote Sens.* 10, 285–306. <https://doi.org/10.3390/rs10200285>.
- Duro, D., Franklin, S., Dubé, M., 2012. Multi-scale object-based image analysis and feature selection of multi-sensor earth observation imagery using random forests. *Int. J. Remote Sens.* 33, 4502–4526. <https://doi.org/10.1080/01431161.2011.649864>.
- Freeman, P., Freeland, R., 2015. Agricultural UAVs in the U.S.: potential, policy, and hype. *Remote. Sens. Appl. Soc. Environ.* 2, 35–43. <https://doi.org/10.1016/j.rsase.2015.10.002>.
- Guyon, I., Elisseeff, A., 2003. An introduction of variable and feature selection. *J. Mach. Learn. Res.* 3, 1157–1182. <https://doi.org/10.1162/153244303322753616>.
- Hall, O., Dahlén, S., Marstorp, H., Archila, M., Oborn, I., Jirström, M., 2018. Classification of maize in complex smallholder farming systems using UAV imagery. *Drones* 2, 22–30. <https://doi.org/10.3390/drones2030022>.
- Han, D., Yang, H., Yang, G., Qiu, C., 2017a. Monitoring model of corn lodging based on Sentinel-1 radar image. 2017 SAR in Big Data Era: models. *Methods Appl. (BIGSARDATA)* 1–5. <https://doi.org/10.1109/BIGSARDATA.2017.8124928>.
- Han, W., Li, G., Yuan, M., Liyuan, Z., Shi, Z., 2017b. Extraction method of maize planting information based on UAV remote sensing technology. *Trans. Chin. Soc. Agric. Mach.* 48, 139–147. <https://doi.org/10.6041/j.issn.1000-1298.2017.01.018>.
- Han, L., Guijun, Y., Feng, H., Zhou, C., Yang, H., Xu, B., Li, Z., Xiaodong, Y., 2018. Quantitative identification of maize lodging-causing feature factors using unmanned aerial vehicle images and a nomogram computation. *Remote Sens.* 10, 1528–1547. <https://doi.org/10.3390/rs10101528>.
- Haralick, R., Shanmugam, K., Dinstein, I., 1973. Textural features for image classification. *IEEE Trans. Syst. Man Cybern. SMC-3*, 610–621.
- Heerden, P.D.R., Singels, A., Paraskevopoulos, A.L., Rossler, R., 2015. Negative effects of lodging on irrigated sugarcane productivity—an experimental and crop modelling assessment. *Field Crops Res.* 180, 135–142. <https://doi.org/10.1016/j.fieldcrops.2015.05.019>.
- Hung, C., Xu, Z., Sukkarieh, S., 2014. Feature learning based approach for weed classification using high resolution aerial images from a digital camera mounted on a UAV. *Remote Sens.* 6, 12037–12054. <https://doi.org/10.3390/rs61212037>.
- Kim, M., Warner, T., Madden, M., Atkinson, D., 2011. Multi-scale GEOBIA with very high spatial resolution digital aerial imagery: scale, texture and image objects. *Int. J. Remote Sens.* 32, 2825–2850. <https://doi.org/10.1080/01431161003745608>.
- Kursa, M., Rudnicki, W., 2010. Feature selection with boruta package. *J. Stat. Softw.* 36, 1–13. <https://doi.org/10.18637/jss.v036.i11>.
- Laliberte, A., Rango, A., 2009. Texture and scale in object-based analysis of subdecimeter resolution unmanned aerial vehicle (UAV) imagery. *IEEE Trans. Geosci. Remote. Sens.* 47, 761–770. <https://doi.org/10.1109/TGRS.2008.2009355>.
- Li, X., 2019a. Advances in research of lodging and evaluation in sugarcane. *Appl. Ecol. Environ. Res.* 17, 6095–6105. https://doi.org/10.15666/aeer/1703_60956105.
- Li, X., 2019b. Evaluation of lodging resistance in sugarcane (*saccharum* spp. *hybrid*) germplasm resources. *Appl. Ecol. Environ. Res.* 17, 6107–6116. https://doi.org/10.15666/aeer/1703_61076116.
- Li, Y., Yang, L.-T., 2015. Sugarcane agriculture and sugar industry in China. *Sugar Tech.* 17, 1–8. <https://doi.org/10.1007/s12355-014-0342-1>.
- Liang, Y., Yu, S., Chen, Z., Zhao, Y., Deng, J., Jiang, W., 2020. Climatic change impacts on Chinese sugarcane planting: benefits and risks. *Phys. Chem. Earth Parts A/B/C* 116, 102856–102864. <https://doi.org/10.1016/j.pce.2020.102856>.
- Liu, H., Yang, G., Zhu, H., 2014. The extraction of wheat lodging area in UAV's image used spectral and texture features. *Appl. Mech. Mater.* 651–653, 2390–2393. <https://doi.org/10.4028/www.scientific.net/AMM.651-653.2390>.
- Liu, T., Li, R., Zhong, X., Jiang, M., Jin, X., Zhou, P., Liu, S., Sun, C., Guo, W., 2018. Estimates of rice lodging using indices derived from UAV visible and thermal infrared images. *Agric. For. Meteorol.* 252, 144–154. <https://doi.org/10.1016/j.agrformet.2018.01.021>.
- Lu, B., He, Y., 2018. Optimal spatial resolution of Unmanned Aerial Vehicle (UAV)-acquired imagery for species classification in a heterogeneous grassland ecosystem. *GIsci. Remote. Sens.* 55, 205–220. <https://doi.org/10.1080/15481603.2017.1408930>.
- Luna, I., Lobo, A., 2016. Mapping crop planting quality in sugarcane from UAV imagery: a pilot study in Nicaragua. *Remote Sens.* 8, 500–518. <https://doi.org/10.3390/rs8060500>.
- Ma, L., Fu, T., Blaschke, T., Li, M., Tiede, D., Zhou, Z., Ma, X., Chen, D., 2017. Evaluation of feature selection methods for object-based land cover mapping of unmanned

- aerial vehicle imagery using random forest and support vector machine classifiers. *ISPRS Int. J. Geoinf.* 6, 51–72. <https://doi.org/10.3390/ijgi6020051>.
- Mardanisamani, S., Maleki, F., Kassani, H., S., Rajapaksa, S., Duddu, H., Wang, M., Shirtliffe, S., Ryu, S., Josuttes, A., Zhang, t., Vail, S., Pozniak, C., Parkin, I., Stavness, I., Eramian, M., 2019. Crop Lodging Prediction From UAV-Acquired Images of Wheat and Canola Using a DCNN Augmented With Handcrafted Texture Features. *CVPR*. <https://doi.org/10.1109/CVPRW.2019.00322>, 2019 Workshop.
- Max, K., 2008. Building predictive models in r using the caret package. *J. Stat. Softw.* 28, 1–26. <https://doi.org/10.18637/jss.v028.i05>.
- Müllerová, J., Brůna, J., Bartalos, T., Dvorák, P., Vítková, M., Pysek, P., 2017. Timing is important: unmanned aircraft vs. Satellite imagery in plant invasion monitoring. *Front. Plant Sci.* 8, 1–13. <https://doi.org/10.3389/fpls.2017.00887>.
- Murakami, T., Yui, M., Amaha, K., 2012. Canopy height measurement by photogrammetric analysis of aerial images: application to buckwheat (*Fagopyrum esculentum* Moench) lodging evaluation. *Comput. Electron. Agric.* 89, 70–75. <https://doi.org/10.1016/j.compag.2012.08.003>.
- Niu, L., Feng, S., Ding, W., Li, G., 2016. Influence of speed and rainfall on large-scale wheat lodging from 2007 to 2014 in China. *PLoS One* 11, e0157677–e0157692. <https://doi.org/10.1371/journal.pone.0157677>.
- Pacifici, F., Chini, M., Emery, W., 2009. A neural network approach using multi-scale textural metrics from very high-resolution panchromatic imagery for urban land-use classification. *Remote Sens. Environ.* 113, 1276–1292. <https://doi.org/10.1016/j.rse.2009.02.014>.
- Pajares, G., 2015. Overview and current status of remote sensing applications based on unmanned aerial vehicles (UAVs). *Photogramm. Eng. Remote Sens.* 81, 281–330. <https://doi.org/10.14358/PERS.81.4.281>.
- Rajapaksa, S., Eramian, M., Duddu, H., Wang, M., Shirtliffe, S., Ryu, S., Josuttes, A., Zhang, T., Vail, S., Pozniak, C., Parkin, I., Ieee, 2018. Classification of crop lodging with gray level Co-occurrence matrix. 2018 IEEE Winter Conference on Applications of Computer Vision 251–258. <https://doi.org/10.1109/wacv.2018.00034>.
- Ruiz, L., Recio, J., Fernandez, A., Hermosilla, T., 2011. A feature extraction software tool for agricultural object-based image analysis. *Comput. Electron. Agric.* 76, 284–296. <https://doi.org/10.1016/j.compag.2011.02.007>.
- Shu, M., Zhou, L., Gu, X., Ma, Y., Sun, Q., Guijun, Y., Zhou, C., 2019. Monitoring of maize lodging using multi-temporal Sentinel-1 SAR data. *Adv. Space Res.* 65, 470–480. <https://doi.org/10.1016/j.asr.2019.09.034>.
- Singh, G., Chapman, S., Jackson, P.A., Lawn, R., 2002. Lodging reduces sucrose accumulation of sugarcane in the wet and dry tropics. *Aust. J. Agric. Res.* 53, 1183–1195. <https://doi.org/10.1071/AR02044>.
- Wang, X., Wang, M., Wang, S., Wu, Y., 2015. Extraction of vegetation information from visible unmanned aerial vehicle images. *Trans. Chin. Soc. Agric. Eng.* 31, 152–159. <https://doi.org/10.3969/j.issn.1002-6819.2015.05.022>.
- Wilke, N., Siegmann, B., Klingbeil, L., Burkart, A., Kraska, T., Muller, O., van Doorn, A., Heinemann, D.G.S., 2019. Quantifying lodging percentage and lodging severity using a UAV-Based canopy height model combined with an objective threshold approach. *Remote Sens.* 11, 515–533. <https://doi.org/10.3390/rs11050515>.
- Wu, W., Wang, W., Michael, M., Yao, X., Peng, W., 2019. Cloud-based typhoon-derived paddy rice flooding and lodging detection using multi-temporal Sentinel-1&2. *Front. Earth Sci.* 13, 682–694. <https://doi.org/10.1007/s11707-019-0803-7>.
- Yang, H., Erxue, C., Li, Z., Zhao, C., Guijun, Y., Pignatti, S., Casa, R., Zhao, L., 2015. Wheat lodging monitoring using polarimetric index from RADARSAT-2 data. *Int. J. Appl. Earth Obs. Geoinf.* 34, 157–166. <https://doi.org/10.1016/j.jag.2014.08.010>.
- Yang, M.-D., Huang, K.-S., Kuo, Y.-H., Tsai, H.-P., Lin, L.-M., 2017. Spatial and spectral hybrid image classification for rice lodging assessment through UAV imagery. *Remote Sens.* 9, 583–602. <https://doi.org/10.3390/rs9060583>.
- Yuan, X., Li, H., Han, Y., Chen, J., Chen, X., 2019. Monitoring of sugarcane crop based on time series of sentinel-1 data: a case study of fusui, guangxi. 2019 8th International Conference on Agro-Geoinformatics (Agro-Geoinformatics) 1–5. <https://doi.org/10.1109/Agro-Geoinformatics.2019.8820221>.
- Zhao, L., Yang, J., Li, P., Shi, L., Zhang, L., 2017. Characterizing lodging damage in wheat and canola using Radarsat-2 polarimetric SAR data. *Remote. Sens. Lett.* 8, 667–675. <https://doi.org/10.1080/2150704X.2017.1312028>.
- Zhao, H., Yuan, C., Song, S., Ding, J., Lin, C.-L., Liang, B., Zhang, M., 2019. Use of unmanned aerial vehicle imagery and deep learning UNet to extract rice lodging. *Sensors.* 19, 3859–3872. <https://doi.org/10.3390/s19183859>.